

Solid State Effects on Spin Transitions: Magnetic, Calorimetric, and Mössbauer-Effect Properties of $[\text{Fe}_x\text{Co}_{1-x}(4,4'\text{-bis-1,2,4-triazole})_2(\text{NCS})_2]\cdot\text{H}_2\text{O}$ Mixed-Crystal Compounds

Jean-Pierre Martin,^{1a} Jacqueline Zarembowitch,^{*,1a} Azzedine Bousseksou,^{1b} Ary Dworkin,^{1c} Jaap G. Haasnoot,^{1d} and François Varret^{1b}

Laboratoire de Chimie Inorganique (CNRS, URA 420) and Laboratoire de Chimie Physique des Matériaux Amorphes (CNRS, URA 1104), Université Paris-Sud, 91405 Orsay, France, Département de Recherches Physiques (CNRS, URA 71), Université Pierre et Marie Curie, 75252 Paris Cedex 05, France, and Gorlaeus Laboratories, Leiden University, P.O. Box 9502, 2300 RA Leiden, The Netherlands

Received April 13, 1994[®]

The study of the effects of metal dilution in the solid state on the spin-crossover behavior of $[\text{Fe}(\text{btr})_2(\text{NCS})_2]\cdot\text{H}_2\text{O}$ (btr = 4,4'-bis-1,2,4-triazole), previously carried out on the mixed-crystal series $[\text{Fe}_x\text{Ni}_{1-x}(\text{btr})_2(\text{NCS})_2]\cdot\text{H}_2\text{O}$, was completed on the series $[\text{Fe}_x\text{Co}_{1-x}(\text{btr})_2(\text{NCS})_2]\cdot\text{H}_2\text{O}$ by using magnetic and calorimetric measurements, as well as ⁵⁷Fe Mössbauer-effect spectrometry which provided the possibility of investigating highly diluted samples (down to $x \approx 4.10^{-3}$). These compounds present interesting peculiar properties: their structure is quasi-two-dimensional and the thermally-induced spin transition they exhibit may occur with a hysteresis effect. When cobalt(II) concentration increases, the iron(II) spin-crossover curves become globally smoother and smoother, and the amount of the residual high-spin form which appears at very low temperature for $x \leq 0.4$ gets larger. Moreover, a variation of x from 1.00 to 0.23 is found to result in a lowering of the transition temperatures, which pass from 121 to 98 K in the cooling mode and from 145 to 98 K in the heating mode. The hysteresis width, which is 24 K for $x = 1.00$, vanishes for $x \approx 0.37$. The enthalpy (entropy) change associated with the spin conversion of 1 mol of iron(II) mononuclear entities varies from $\approx 10.0 \text{ kJ}\cdot\text{mol}^{-1}$ ($\approx 76 \text{ J}\cdot\text{K}^{-1}\cdot\text{mol}^{-1}$) for $x = 1.00$ to $\approx 2.0 \text{ kJ}\cdot\text{mol}^{-1}$ ($\approx 17 \text{ J}\cdot\text{K}^{-1}\cdot\text{mol}^{-1}$) for $x = 0.23$. When comparing the data obtained for the related series $[\text{Fe}_x\text{Co}_{1-x}]$ and $[\text{Fe}_x\text{Ni}_{1-x}]$, differences are observed concerning the evolution with x of the transition temperatures and of the hysteresis width, as well as the existence of a residual high-spin fraction at low temperatures. The above findings were accounted for qualitatively by taking into account the relative sizes of Co(II), high-spin Fe(II), and low-spin Fe(II) ions and then quantitatively on the basis of a thermodynamic model.

Introduction

The behavior of spin-crossover systems is governed, in the solid state, by intermolecular interactions, which are responsible for the deviation from the Gibbs–Boltzmann distribution over the vibronic levels of the high-spin (HS) and low-spin (LS) states observed in liquid solutions.^{2–11} Studying the effects of the metal ion dilution in the solid state proved to be a fruitful method to clarify the role of these interactions.^{12–28}

We have previously reported a study of the iron(II) spin transition in the mixed-crystal series $[\text{Fe}_x\text{Ni}_{1-x}(\text{btr})_2(\text{NCS})_2]\cdot\text{H}_2\text{O}$

(btr = 4,4'-bis-1,2,4-triazole), denoted $[\text{Fe}_x\text{Ni}_{1-x}]$, where the nickel(II) ions retain the HS state at any temperature.²⁸ The pure iron compound $[\text{Fe}(\text{btr})_2(\text{NCS})_2]\cdot\text{H}_2\text{O}$, abbreviated as [Fe], exhibits a discontinuous thermally-induced spin transition^{28,29} (80% of the spin conversion occurring within an interval of ≈ 3 K), complete at both high and low temperatures, and presenting a wide hysteresis of 24 K ($T_c^\downarrow = 121 \text{ K}$ and $T_c^\uparrow = 145 \text{ K}$,²⁸ T_c^\downarrow and T_c^\uparrow corresponding to the temperatures at which the HS fraction, n_{HS} , is equal to 0.5 in the cooling and the heating

[®] Abstract published in *Advance ACS Abstracts*, November 15, 1994.

- (1) (a) Laboratoire de Chimie Inorganique, Université Paris-Sud; (b) Département de Recherches Physiques, Université Pierre et Marie Curie; (c) Laboratoire de Chimie Physique des Matériaux Amorphes, Université Paris-Sud; (d) Gorlaeus Laboratories, Leiden University.
- (2) Gütllich, P. *Structure and Bonding* **1981**, *44*, 83.
- (3) König, E.; Ritter, G.; Kulshreshtha, S. K. *Chem. Rev.* **1985**, *85*, 219.
- (4) König, E. *Progr. Inorg. Chem.* **1987**, *35*, 527.
- (5) Beattie, J. K. *Adv. Inorg. Chem.* **1988**, *32*, 1.
- (6) Bacci, M. *Coord. Chem. Rev.* **1988**, *86*, 245.
- (7) Toftlund, H. *Coord. Chem. Rev.* **1989**, *67*, 108.
- (8) Gütllich, P.; Hauser, A. *Coord. Chem. Rev.* **1990**, *97*, 1.
- (9) Hauser, A. *Coord. Chem. Rev.* **1991**, *111*, 275.
- (10) König, E. *Structure and Bonding* **1991**, *76*, 51.
- (11) Zarembowitch, J. *New J. Chem.* **1992**, *16*, 255.
- (12) Hendrickson, D. N.; Haddad, M. S.; Federer, W. D.; Lynch, M. W. (*IUPAC*) *Coordination Chemistry-21*; Laurent, J. P., Ed.; Pergamon Press: Oxford and New York, 1981; p 75.
- (13) Haddad, M. S.; Federer, W. D.; Lynch, M. W.; Hendrickson, D. N. *J. Am. Chem. Soc.* **1980**, *102*, 1468.
- (14) Haddad, M. S.; Federer, W. D.; Lynch, M. W.; Hendrickson, D. N. *Inorg. Chem.* **1981**, *20*, 131.
- (15) Zelentsov, V. V.; Gabdrakhmanov, M. N.; Sobolev, S. S. *Khim. Fiz.* **1986**, *5*, 1216.

- (16) Sorai, M.; Ensling, J.; Gütllich, P. *Chem. Phys.* **1976**, *18*, 199.
- (17) Gütllich, P.; Link, R.; Steinhäuser, H. G. *Inorg. Chem.* **1978**, *17*, 2509.
- (18) Kambara, T. *J. Phys. Soc. Jpn.* **1980**, *49*, 1806.
- (19) Spiering, H.; Meissner, E.; Köppen, H.; Müller, E. W.; Gütllich, P. *Chem. Phys.* **1982**, *68*, 65.
- (20) Sanner, I.; Meissner, E.; Köppen, H.; Spiering, H.; Gütllich, P. *Chem. Phys.* **1984**, *86*, 227.
- (21) Adler, P.; Wiehl, L.; Meissner, E.; Köhler, C. P.; Spiering, H.; Gütllich, P. *J. Phys. Chem. Solids* **1987**, *48*, 517.
- (22) Jakobi, R.; Spiering, H.; Wiehl, L.; Gmelin, E.; Gütllich, P. *Inorg. Chem.* **1988**, *27*, 1823.
- (23) Köhler, C. P.; Jakobi, R.; Meissner, E.; Wiehl, L.; Spiering, H.; Gütllich, P. *J. Phys. Chem. Solids* **1990**, *51*, 239.
- (24) Jakobi, R.; Spiering, H.; Gütllich, P. *J. Phys. Chem. Solids* **1992**, *53*, 267.
- (25) Rao, P. S.; Reuveni, A.; Mc Garvey, B. R.; Ganguli, P.; Gütllich, P. *Inorg. Chem.* **1981**, *20*, 204.
- (26) Rao, P. S.; Mc Garvey, B. R.; Ganguli, P. *Inorg. Chem.* **1981**, *20*, 3682.
- (27) Ganguli, P.; Gütllich, P.; Müller, E. W. *Inorg. Chem.* **1982**, *21*, 3429.
- (28) Martin, J.-P.; Zarembowitch, J.; Dworkin, A.; Haasnoot, J. G.; Codjovi, E. *Inorg. Chem.* **1994**, *33*, 2617.
- (29) Vreugdenhil, W.; Van Diemen, J. H.; De Graaf, R. A. G.; Haasnoot, J. G.; Reedijk, J.; Van der Kraan, A. M.; Kahn, O.; Zarembowitch, J. *Polyhedron* **1990**, *9*, 2971.

Table 1. Elemental Analysis Data (%) and Molecular Weights (g) for the Mixed-Crystal Series $[\text{Fe}_x\text{Co}_{1-x}(\text{btr})_2(\text{NCS})_2]\cdot\text{H}_2\text{O}$

x	M	C		H		N		S		Fe	Co
		obsd	calcd	obsd	calcd	obsd	calcd	obsd	calcd		
1.00	462.26	26.02	25.96	2.03	2.16	42.22	42.40	14.02	13.85	11.52	0.00
0.96	462.38	26.08	25.95	1.95	2.16	42.54	42.39	14.19	13.84	11.38	0.49
0.80	462.88	25.85	25.92	2.12	2.16	43.37	42.34	13.74	13.83	9.80	2.55
0.75	463.03	26.48	25.92	2.03	2.16	42.86	42.33	13.96	13.82	8.86	3.11
0.59	463.55	25.77	25.89	2.14	2.16	43.50	42.28	13.81	13.81	7.04	5.25
0.54	463.68	26.59	25.88	2.07	2.16	42.84	42.27	13.75	13.80	6.44	5.88
0.39	464.14	25.75	25.85	2.10	2.15	43.45	42.23	13.75	13.79	4.64	7.56
0.35	464.26	26.59	25.85	2.16	2.15	42.68	42.22	13.77	13.79	4.20	8.29
0.23	464.60	25.80	25.83	2.13	2.15	43.17	42.19	13.77	13.78	2.95	9.52
0.20	464.66	25.89	25.83	2.06	2.15	41.52	42.18	13.86	13.77	2.46	9.47
0.05	465.19	26.03	25.80	2.30	2.15	42.05	42.13	13.99	13.76	0.52	11.03
0.01	465.31	26.32	25.79	2.27	2.15	42.63	42.12	13.96	13.75	0.13	11.28
0.004	465.33	26.49	25.79	2.26	2.15	43.06	42.12	13.85	13.75	0.04	11.49
0.00	465.34	26.25	25.79	2.25	2.15	42.86	42.12	13.85	13.75	0.00	11.49

modes, respectively). It has been shown²⁸ that dilution (i) reduces the cooperativity of the phenomenon, as a result of the removal of iron(II) ions away from each other, and (ii) introduces interactions between these ions and the additional metal ions. The former effect was accounted for by a smoothing of the transition curves and a narrowing of the hysteresis loops with decreasing iron(II) concentration, while the latter was found to mainly modify the values of the transition enthalpy and entropy and, consequently, to result in transition temperature changes. The relative sizes of the metal ions were shown to take a large part in the magnitude of these effects. The ionic radius of Ni(II) (83 pm) is nearly equal to the mean value of the ionic radii of Fe(II) in the HS and the LS states (92 and 75 pm, respectively). On the other hand, the cobalt(II) ion has a ionic radius (88.5 pm) close to the one of iron(II) in the HS state. It follows that the study of mixed-crystal compounds of the type $[\text{Fe}_x\text{Co}_{1-x}(\text{btr})_2(\text{NCS})_2]\cdot\text{H}_2\text{O}$ ($[\text{Fe}_x\text{Co}_{1-x}]$) is expected to be particularly fruitful, for a comparison between the behaviors of $[\text{Fe}_x\text{Co}_{1-x}]$ and $[\text{Fe}_x\text{Ni}_{1-x}]$ species should provide original information concerning the effects of metal dilution on the spin transition. Moreover the structure of $[\text{Co}(\text{btr})_2(\text{NCS})_2]\cdot\text{H}_2\text{O}$ ³⁰ ($[\text{Co}]$) is known to be isomorphous with that of $[\text{Fe}]$. Both consist of layers of six-coordinate metal ions linked to each other, in the equatorial plane, through the bis-triazole ligands acting as single bridges. The thiocyanate groups are N-bonded and *trans*-oriented with regard to this plane. The water molecules are located between the layers, each of them being weakly hydrogen-bonded to two bis-triazole ligands lying in the two neighboring planes.

In the present paper, we report an experimental study of the dilution effects in $[\text{Fe}_x\text{Co}_{1-x}]$ complexes, carried out on the basis of variable temperature magnetic susceptibility, Mössbauer spectrometry, and differential scanning calorimetry (DSC) measurements. As in the preceding investigation, the experimental data were treated through an adaptation of the Slichter and Drickamer thermodynamic model.³¹

Experimental Section

Materials. The bis-triazole ligand was synthesized as described elsewhere.³²

The complexes were prepared according to a procedure derived from that previously adopted for obtaining the pure compounds or similar mixed-crystal species:^{28–30,32,33} the hot aqueous solutions (80 °C) containing bis-triazole ligand, ammonium thiocyanate, iron(II) chloride,

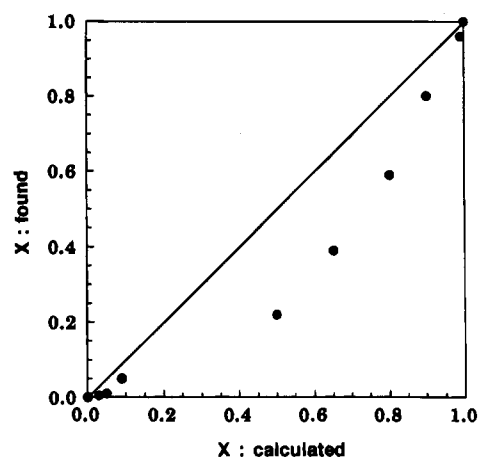


Figure 1. Iron fraction x obtained from elemental analysis vs iron fraction calculated from the iron/cobalt ratio used for the synthesis. The full line corresponds to the hypothetical situation where x found = x calculated.

and/or cobalt(II) chloride were stirred and then slowly cooled to room temperature. For the species with very low iron concentration (characterized by $x \leq 0.1$), the study of which was performed by Mössbauer spectrometry, the syntheses were carried out by using ⁵⁷Fe-enriched iron, in order to get at least 100 μg of ⁵⁷Fe in a sample of typically 100 mg. This amount is required to obtain an acceptable signal/noise ratio. All the elemental analysis data, and the values of iron fractions (x) and molecular weights (M_x) deduced from these data, are collected in Table 1.

Iron fraction values were determined from the iron and cobalt concentrations provided by elemental analyses, according to the method previously used in the case of the related mixed-crystals series $[\text{Fe}_x\text{Ni}_{1-x}]$.²⁸ The discrepancies between the values thus obtained and those calculated from the relative amounts of the metal salts used for the syntheses (see Figure 1) are found to be more pronounced than in the $[\text{Fe}_x\text{Ni}_{1-x}]$ series.

Magnetic Measurements. These measurements were performed on crystalline samples of typical weight 5 mg, over the temperature range 295–50 K, using a Faraday-type magnetometer equipped with an Oxford Instruments helium continuous-flow cryostat. The independence of the susceptibility with regard to the applied magnetic field was checked for each compound at room temperature. Mercury tetrakis(thiocyanato)cobaltate was used as a susceptibility standard. Diamagnetism corrections on the susceptibility values were taken as $-150 \cdot 10^{-6} \text{ cm}^3 \cdot \text{mol}^{-1}$ for all compounds. Temperature was varied at the rate of $1 \text{ K} \cdot \text{min}^{-1}$ in the cooling mode and $\approx 0.5 \text{ K} \cdot \text{min}^{-1}$ in the heating mode.

Thermogravimetric analysis experiments have shown that the higher the iron concentration, the easier the loss of water molecules. When x increases from 0.00 to 0.40 and then to 0.80, the temperature at which water is completely removed decreases from 95 to 85 °C and then to 72 °C. In the absence of water, iron(II) is in the HS state at any

(30) Vreugdenhil, W.; Gorter, S.; Haasnoot, J. G.; Reedijk, J. *Polyhedron* **1985**, *4*, 1769.

(31) Slichter, C. P.; Drickamer, H. G. *J. Chem. Phys.* **1972**, *56*, 2142.

(32) Haasnoot, J. G.; Groeneveld, W. L. *Z. Naturforsch.* **1979**, *34b*, 1500.

(33) Vreugdenhil, W.; Haasnoot, J. G.; Kahn, O.; Thuéry, P.; Reedijk, J. *J. Am. Chem. Soc.* **1987**, *109*, 5272.

Table 2. $\chi_{\text{Fe}}T$ Values at Room Temperature for Various $[\text{Fe}_x\text{Co}_{1-x}]$ Compounds

x	$\chi_{\text{Fe}}T$ ($\text{cm}^3\text{mol}^{-1}\text{K}$)	x	$\chi_{\text{Fe}}T$ ($\text{cm}^3\text{mol}^{-1}\text{K}$)
1.00	3.63	0.54	3.96
0.96	3.83	0.39	3.62
0.80	3.66	0.23	5.05
0.75	3.88	0.20	3.53
0.59	3.70		

temperature. So, a special procedure was used upon magnetic susceptibility measurements in order to prevent the loss of water: the sample was submitted to a primary vacuum for 1 min at 160 K and then kept under 1 atm of helium pressure.

Mössbauer Spectrometry Experiments. The Mössbauer spectra were obtained on a constant-acceleration spectrometer with a 25-mCi source of ^{57}Co in a rhodium matrix. The calibration was made with a metallic iron foil at room temperature. The experimental line width was typically 0.22 mm s^{-1} . The absorber was a sample of $\approx 100 \text{ mg}$ of $[\text{Fe}_x\text{Co}_{1-x}(\text{btr})_2(\text{NCS})_2]\cdot\text{H}_2\text{O}$ polycrystalline powder, enclosed in a capsule $\approx 1 \text{ cm}$ in diameter, the size of which had been determined in order to get an optimal absorption. The compounds characterized by a very low iron(II) concentration ($x \leq 0.10$) were doped with ^{57}Fe . Temperature was varied, very slowly, in the range 295 to 4.2 K, using a helium continuous-flow cryostat Oxford CF-300 monitored by a servocontrol device (accuracy, $\pm 0.1 \text{ K}$). Samples were kept under helium at a pressure of 1 atm. The typical counting time was ca. 6 h. A least-squares computer program was used to fit the Mössbauer parameters.

DSC Measurements. The differential scanning calorimetry analysis was conducted on a Perkin-Elmer DSC-2 instrument, a home-made cooling system allowing the temperature to be lowered to 83 K.³⁴ The purging gas was helium. Temperature and enthalpy were calibrated using the melting transition (279.69 K , 2670 J mol^{-1}) and the crystal to crystal transition (186.70 K , 6740 J mol^{-1}) of a cyclohexane sample. Temperature values were determined with a $\pm 0.5 \text{ K}$ accuracy, and enthalpy values were estimated with an experimental uncertainty of $\pm 2\%$ for a scan rate of 10 K min^{-1} . Samples, the masses of which were typically 5–10 mg, were sealed in aluminium pans.

Results

Magnetic Data. The evolution of $\chi_{\text{exp}}T$ (χ_{exp} = measured magnetic susceptibility for 1 mol of $[\text{Fe}_x\text{Co}_{1-x}]$ entities and T = temperature) as a function of temperature was determined for each compound. χ_{exp} is the sum of the contributions of iron(II) ions and cobalt(II) ions:

$$\chi_{\text{exp}}T = x\chi_{\text{Fe}}T + (1-x)\chi_{\text{Co}}T \quad (1)$$

then

$$\chi_{\text{Fe}}T = \frac{\chi_{\text{exp}}T - (1-x)\chi_{\text{Co}}T}{x} \quad (2)$$

As iron(II) ions in the LS state are diamagnetic, $\chi_{\text{Fe}}T$ is proportional to the HS fraction n_{HS} . So, all the samples being entirely in the HS form ($n_{\text{HS}} = 1$) at room temperature, as shown by the Mössbauer spectra, the n_{HS} value at a given temperature T can be determined by dividing the value of $\chi_{\text{Fe}}T$ at T by the one at room temperature given in Table 2. When the iron concentration decreases, the error on $\chi_{\text{Fe}}T$ values becomes more and more important since $\chi_{\text{exp}}T$ and $(1-x)\chi_{\text{Co}}T$ get closer. Nevertheless, the trend of the evolution of these values can be considered meaningful.

Figure 2 shows the n_{HS} vs T curves obtained in the cooling and the heating modes for several mixed compounds. When x decreases, (i) the slope of the curves around the point of inflection diminishes—first very slightly from $x = 1.00$ to $x \approx$

0.50 and then more and more rapidly—which indicates a reduction of the spin-crossover cooperativity; (ii) the hysteresis loop is shifted toward low temperatures and gets narrower so far as to vanish for $x \approx 0.37$; and (iii) a residual HS fraction (r_{HS}), the amount of which increases with dilution, is observed at very low temperature. The first and third effects are more clearly evidenced if the n_{HS} vs T curves obtained for a representative set of x values in the cooling mode on the one hand, and in the heating mode on the other hand, are collected in two separate figures (see Figure 3a,b). The residual HS fraction at 60 K is found to vary from a value lower than 0.1 for $0.5 < x < 1.0$ to 0.36 for $x = 0.23$. We shall see hereafter, from Mössbauer spectrometry data, that this latter value is highly overestimated, as a consequence of the large uncertainty on n_{HS} for low iron concentrations (vide supra); nevertheless, the trend observed for the variation of r_{HS} as a function of x will be corroborated.

Owing to the existence of a residual HS fraction, the transition temperatures in the cooling mode ($T_c\downarrow$) and in the heating mode ($T_c\uparrow$) have to be redefined: they are taken as the temperatures at which the high-spin fraction is equal to $(1 + r_{\text{HS}})/2$. They both decrease with iron concentration (see Figure 4). When x changes from 1.00 to 0.23, $T_c\uparrow$ varies from 145 to 98 K and $T_c\downarrow$ from 121 to 98 K. If we assume as a first approximation that the transition temperature T_c is defined by $(T_c\downarrow + T_c\uparrow)/2$, the value of T_c is found to decrease from 133 to 98 K between the same limits. The hysteresis width, which is 24 K for $x = 1.00$, becomes 2 K for $x \approx 0.39$ and is no more detectable for $x < \approx 0.37$.

So, magnetic measurements proved to be a suitable technique to provide evidence for dilution effects in the mixed-crystals series $[\text{Fe}_x\text{Co}_{1-x}]$. However, as seen above, these effects cannot be accurately detected when the correction of susceptibility due to the presence of cobalt(II) ions is too large compared to the susceptibility of iron(II) ions, i.e. in the case of highly diluted species. Mössbauer spectrometry was used to study these compounds (enriched with ^{57}Fe), as well as to check the results obtained from magnetism experiments for some compounds with high x values.

Mössbauer Spectra. At room temperature, whatever x may be, the Mössbauer spectra exhibit a single doublet with typical values of $2.80\text{--}2.85 \text{ mm s}^{-1}$ for the quadrupole splitting (ΔE_Q) and $1.04\text{--}1.05 \text{ mm s}^{-1}$ for the isomer shift (δ). These values are characteristic of iron(II) in the HS state. When the temperature is lowered, a new peak appears between the two HS lines, the intensity of which increases on cooling, up to a limit depending on x . For spectra simulation, this peak was assumed to be formed by two unresolved components. At 4.2 K, the relevant Mössbauer parameters were estimated to be $\Delta E_Q = 0.11\text{--}0.15 \text{ mm s}^{-1}$ and $\delta = 0.52\text{--}0.54 \text{ mm s}^{-1}$, which is typical for iron(II) in the low-spin state. The values of ΔE_Q and δ , characterizing the HS doublet at room temperature and 4.2 K and the LS doublet at 4.2 K for all the samples, are detailed in Table 3. At a given temperature, they are found to be independent of x , within the experimental errors, as was already observed in previous studies on dilution effects.^{17,20,27}

A selection of the Mössbauer spectra obtained for the undiluted complex [Fe] and the highly-diluted species $[\text{Fe}_{0.05}\text{Co}_{0.95}]$ at some representative temperatures, in the heating mode, is shown in Figure 5. It clearly appears that the behavior of the two compounds is different. In the latter case, the HS/LS ratio varies much more slowly as a function of temperature than in the former case, the transition temperature is lower, and a noticeable amount of HS form is retained at very low tempera-

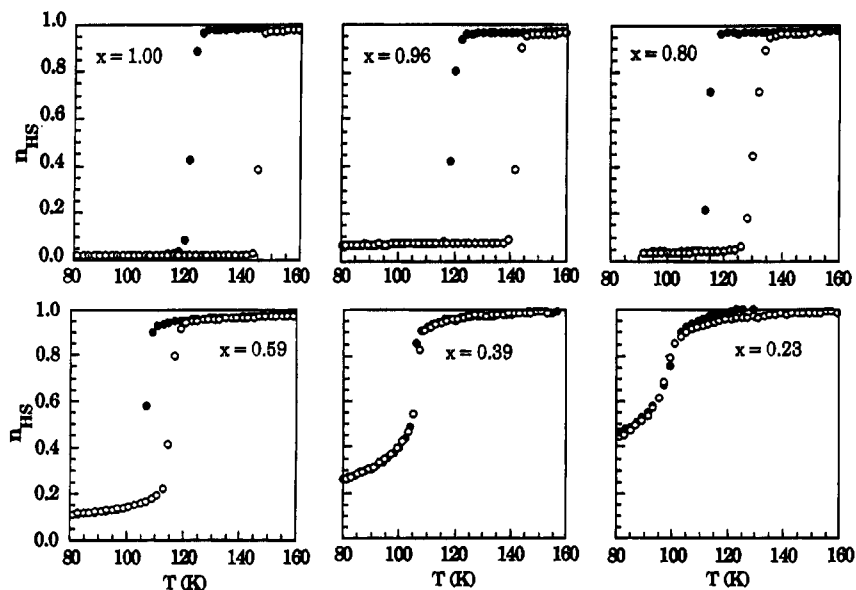


Figure 2. r_{HS} vs T curves obtained, for different x values, from magnetic susceptibility measurements in the cooling (●) and heating (○) modes.

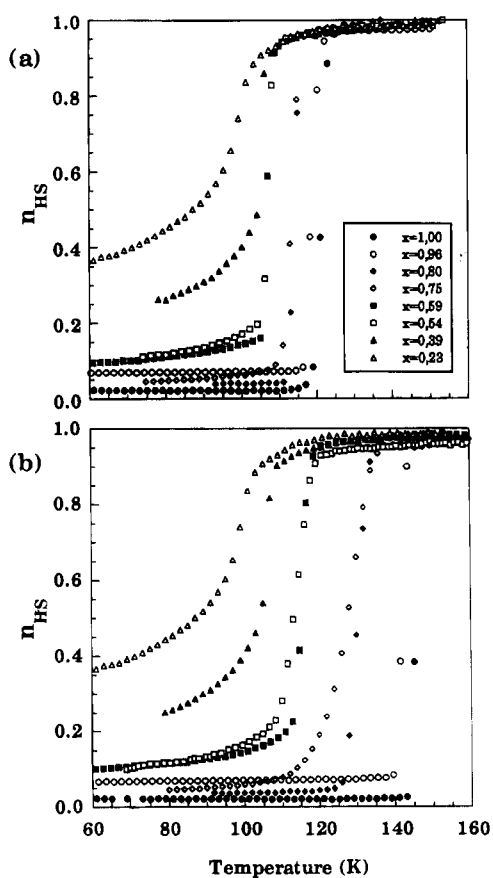


Figure 3. Evolution as a function of x of the r_{HS} vs T curves obtained (a) in the cooling mode and (b) in the heating mode from magnetic susceptibility measurements.

ture. This corroborates the trends observed from magnetic susceptibility measurements.

The evolution of the HS residual fraction at 4.2 K as a function of iron concentration is shown in Figure 6. These data are more accurate than those deduced from magnetism experiments, since they do not require corrections for cobalt(II) ions. r_{HS} is found not to exceed 2% from $x = 1.0$ to $x \approx 0.6$ and then to increase with dilution so far as to reach 15.6(5)% for $x = 0.01$. The experimental r_{HS} value corresponding to $x = 0.23$ is likely to be somewhat overestimated, because the temperature

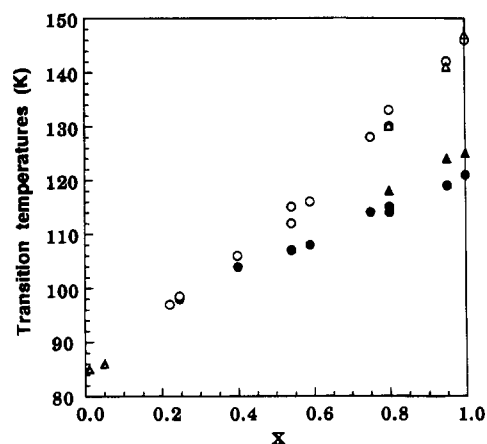


Figure 4. Evolution as a function of x of the transition temperatures in the cooling (●, ▲) and heating (○, △) modes, derived from magnetic susceptibility measurements (circles) and Mössbauer spectra (triangles).

Table 3. Isomer Shift (δ) Referred to Metallic Iron at Room Temperature and Quadrupole Splitting (ΔE_{Q}) Derived from the Least Squares Simulated Mössbauer Spectra, for the HS Doublet of Iron(II) at Room Temperature and at 4.2 K and for the LS Doublet at 4.2 K

x	room temperature (HS state)		$T = 4.2$ K (HS state)		$T = 4.2$ K (LS state)	
	δ ($\text{mm}\cdot\text{s}^{-1}$)	ΔE_{Q} ($\text{mm}\cdot\text{s}^{-1}$)	δ ($\text{mm}\cdot\text{s}^{-1}$)	ΔE_{Q} ($\text{mm}\cdot\text{s}^{-1}$)	δ ($\text{mm}\cdot\text{s}^{-1}$)	ΔE_{Q} ($\text{mm}\cdot\text{s}^{-1}$)
1.00	1.047	2.809			0.524	0.149
0.96	1.042	2.804				
0.80	1.091	2.961			0.527	0.133
0.59	1.042	2.829			0.534	0.138
0.39	1.037	2.822	1.218	3.42	0.537	0.126
0.23			1.209	3.40	0.539	0.123
0.05	1.121	3.119	1.164	3.25	0.520	0.114
0.01	1.039	2.825	1.158	3.25	0.519	0.121
0.004	1.053	2.851	1.161	3.30	0.522	0.122

was lowered rather more rapidly for this compound than for the other samples. Now, in the present series, r_{HS} was shown to strongly depend on the cooling rate: as an example, quenching the sample with $x = 0.01$ in cold helium gas led to trap $\approx 50\%$ of HS form. It is worth pointing out that, in the series $[\text{Fe}_x\text{Ni}_{1-x}]$, no noticeable amount of HS residual fraction was observed at very low temperature, even for the most diluted species.²⁸

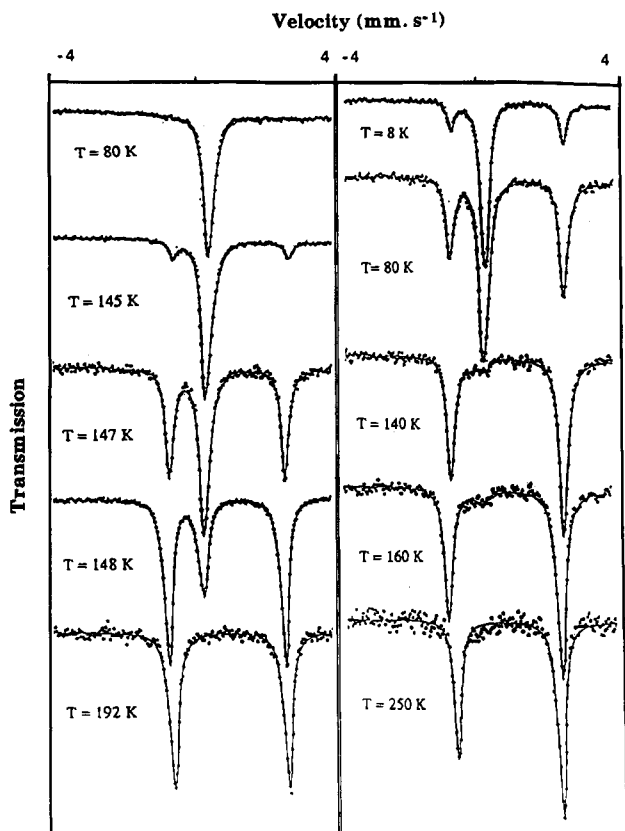


Figure 5. Mössbauer spectra, for a representative set of temperatures, of the compounds characterized by $x = 1.00$ (left) and $x = 0.05$ (right). Measurements were performed in the heating mode.

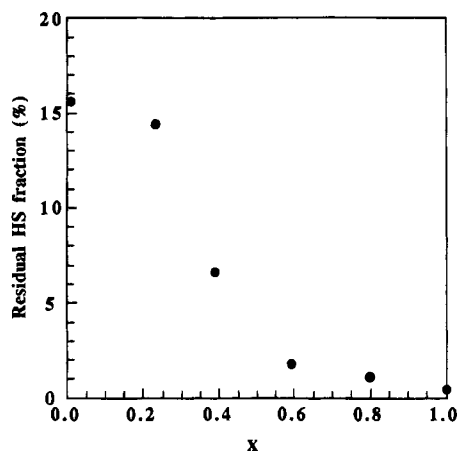


Figure 6. Evolution as a function of x of the residual HS fraction at very low temperature (4.2 K), derived from Mössbauer spectrometry data.

The transition temperatures deduced from Mössbauer spectra are plotted, in Figure 4, as a function of dilution. For low x values, they complete the data provided by the magnetic measurements. In the case of concentrated samples, they are in agreement with these data in the heating mode, whereas they are somewhat higher in the cooling mode. This trend can be observed in Figure 7, which shows the spin-transition hysteresis loops obtained for $[\text{Fe}_{0.80}\text{Co}_{0.20}]$ from both magnetism and Mössbauer spectrometry experiments. It can be easily explained if one notices that, when several hysteresis loops were swept successively on a given sample, T_c^\dagger and T_c^\ddagger were found to shift toward higher temperatures (probably as a result of the damage of crystals upon the spin change), the limit being reached after two cycles. Now, given the experimental procedures, the decreasing temperature branch, in Figure 7, corresponds to the

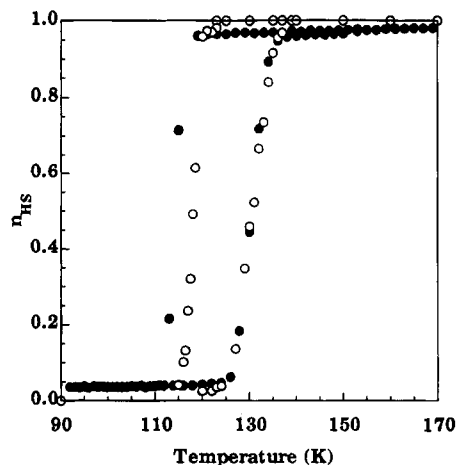


Figure 7. Comparison of the n_{HS} vs T curves obtained in the cooling and heating modes for $[\text{Fe}_{0.80}\text{Co}_{0.20}]$ from magnetic susceptibility (●) and Mössbauer spectrometry (○) measurements.

first spin transition presented by the sample in magnetism experiments and to the third one in Mössbauer spectrometry experiments, while the increasing branch is related to the second spin transition in both techniques.

From Figure 4, the transition temperature T_c appears to vary nearly linearly with iron concentration. A linear behavior of T_c as a function of x was also reported in the case of the mixed compounds $[\text{Fe}_x\text{Zn}_{1-x}(2\text{-pic})_3]\text{Cl}_2\cdot\text{EtOH}$ with $0.2 \leq x \leq 1.0$ ¹⁶ (2-pic = 2-picolyamine); on the other hand, a deviation from linearity was found for the samples with $x \leq 0.15$.¹⁷ Similar results were obtained for $[\text{Fe}_x\text{Co}_{1-x}(2\text{-pic})_3]\text{Cl}_2\cdot\text{EtOH}$ complexes.²⁰ In the series $[\text{Fe}_x\text{Zn}_{1-x}(2\text{-pic})_3]\text{Cl}_2\cdot\text{MeOH}$, the linearity was observed down to $x = 0.01$.²¹

DSC Data. The thermodynamic parameters associated with the spin conversions were determined experimentally from differential scanning calorimetry measurements. In the thermograms, the peak area corresponds to an enthalpy. For each $[\text{Fe}_x\text{Co}_{1-x}]$ complex, we have calculated the enthalpy change ΔH related to the conversion of 1 mol of [Fe] mononuclear entities, according to the relation

$$\Delta H = \frac{\Delta H_{\text{exp}} M_x}{x(1 - r_{\text{HS}})} \quad (3)$$

where ΔH_{exp} , the experimental value of enthalpy related to the mass unit of the sample, was directly obtained from the DSC data processing program.

As defined before, T_c is the temperature at which ΔG vanishes. So, the entropy variation ΔS was determined from $\Delta S = \Delta H/T_c$. Experimental errors vary from $\approx 5\%$ ($x = 1$) to $\approx 30\%$ ($x = 0.23$) for ΔH and are somewhat larger for ΔS . The thermograms depicted in Figure 8, obtained in the heating mode, are related to the same mass of various $[\text{Fe}_x\text{Co}_{1-x}]$ complexes. As dilution increases, the peaks are shifted toward low temperatures and, as expected, their amplitude decreases. The latter effect shows the limit of the method, which is of the same order as that observed in the case of the related series $[\text{Fe}_x\text{Ni}_{1-x}]$,²⁸ for $x \leq 0.2$, the signal cannot be distinguished from the noise.

Figure 9 represents the evolution of ΔH as a function of x . ΔH decreases continuously from $\approx 10.0 \text{ kJ}\cdot\text{mol}^{-1}$ for $x = 1.00$ to $\approx 2.0 \text{ kJ}\cdot\text{mol}^{-1}$ for $x = 0.23$. Figure 10 shows the same behavior for the entropy change. ΔS decreases from $\approx 76 \text{ J}\cdot\text{K}^{-1}\cdot\text{mol}^{-1}$ for $x = 1.00$ to $\approx 17 \text{ J}\cdot\text{K}^{-1}\cdot\text{mol}^{-1}$ for $x = 0.23$. The two curves are different from those obtained with $[\text{Fe}_x\text{Ni}_{1-x}]$ complexes,²⁸ which present a flat portion from $x = 1$ to $x \approx 0.7$.

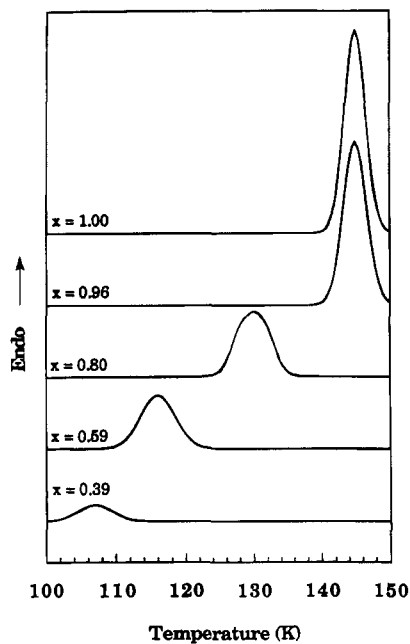


Figure 8. DSC curves, in the heating mode, referring to the spin conversion of the same mass of various $[\text{Fe}_x\text{Co}_{1-x}]$ complexes. For clarity, the curves have been translated vertically.

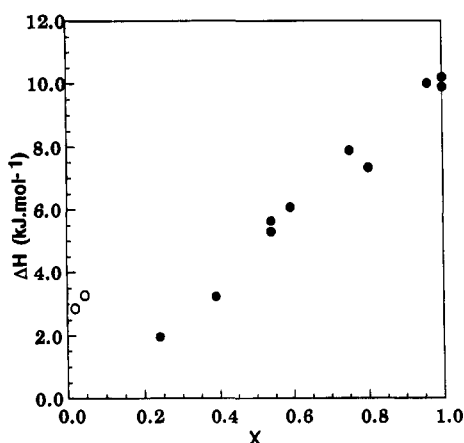


Figure 9. Evolution as a function of x of the transition enthalpy related to 1 mol of $[\text{Fe}]$ entities: (●), DSC data; (○), data deduced from Mössbauer spectrometry measurements.

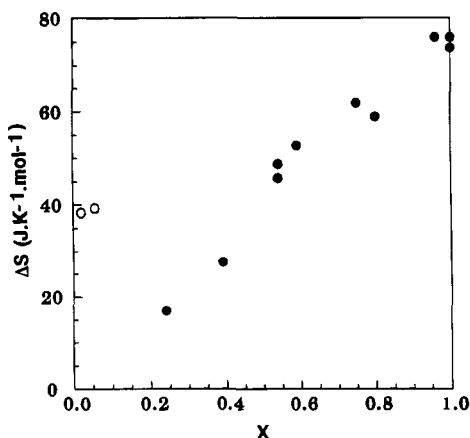


Figure 10. Evolution as a function of x of the transition entropy related to 1 mol of $[\text{Fe}]$ entities: (●), data deduced from DSC measurements; (○), data deduced from Mössbauer spectrometry measurements.

In the case of the highly diluted samples $x = 0.05$ and $x = 0.01$, ΔH and ΔS could be estimated using the n_{HS} values deduced from variable-temperature Mössbauer spectrometry

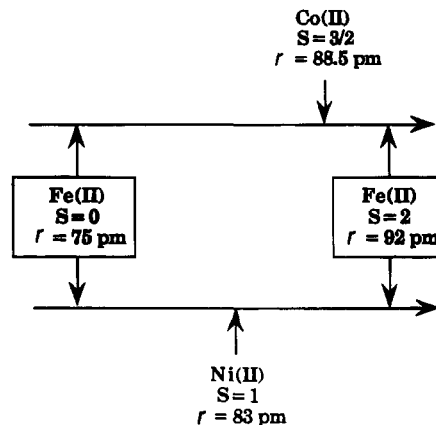


Figure 11. Comparison of the ionic radii of HS and LS iron(II) with those of HS cobalt(II) and HS nickel(II).

data. For such dilutions, it has been shown previously²⁸ that the probability for an iron ion to be only surrounded by metal ions of different nature is very high (at least 83%). So, the intermolecular interactions between spin-changing ions are likely to be negligible and, as a first approximation, the law of mass action can be considered obeyed. This may be written, taking into account the residual high-spin fraction at low temperature, as

$$\ln \left[\frac{1 - n_{\text{HS}}}{n_{\text{HS}} - r_{\text{HS}}} \right] = \frac{\Delta H}{RT} - \frac{\Delta S}{R} \quad (4)$$

Linear regressions on Arrhenius-type plots led to the following values: $\Delta H = 3.25 \pm 0.05$ and $2.90 \pm 0.05 \text{ kJ}\cdot\text{mol}^{-1}$ and $\Delta S = 39.5 \pm 0.5$ and $38.5 \pm 0.5 \text{ J}\cdot\text{K}^{-1}\cdot\text{mol}^{-1}$, for $x = 0.05$ and 0.01 , respectively. These data are reported as open circles on Figures 9 and 10. Though they are of the same order of magnitude as those obtained from DSC measurements for the most diluted samples, the ΔH and ΔS values thus determined are found to be higher. This may be partly accounted for by the significant uncertainty on the experimental ΔH values, which are expected to be all the more underestimated when x is low.

Discussion

From magnetic susceptibility measurements and Mössbauer spectra, iron(II) dilution was found to result in a global smoothing of the spin transition as a function of temperature, a reduction and then a vanishing of the hysteresis loop, a decrease of the transition temperatures T_c^\downarrow and T_c^\uparrow , and an increase of the residual HS fraction at very low temperature. Moreover, DSC measurements allowed one to get the evolution of ΔH and ΔS as a function of x .

Since dilution effects are expected to result from the separation of the spin-crossover $[\text{Fe}]$ groups from each other and the establishment of interactions between these groups and $[\text{Co}]$ entities, they are likely to depend on the relative sizes of the two metal ions.

The fact that the ionic radius of cobalt(II) is very close to that of iron(II) in the HS state, while the ionic radius of nickel(II) is nearly equal to the mean value of the ionic radii of iron(II) in the HS and LS states (see Figure 11), is expected to be mainly responsible for the difference in behavior of the series $[\text{Fe}_x\text{Ni}_{1-x}]$ ²⁸ and $[\text{Fe}_x\text{Co}_{1-x}]$.

Let us consider the introduction of iron(II) ions in a crystal of $[\text{Co}]$. Two cases have to be distinguished. If the iron(II) ions are in the HS state, they are submitted to a positive pressure from their surroundings. Their LS form is then stabilized. However, this local effect is expected to be of small importance,

given the fact that the sizes of the two types of metal ions differ only slightly. On the other hand, if the iron(II) ions are in the LS state, they are submitted to a negative pressure from their surroundings, which stabilizes their HS form. This effect is now expected to be significant, owing to the large difference between the ionic radii of the two metals. In both cases, the presence of cobalt ions leads to a destabilization of the initial spin state of iron ions. However, the latter effect being much more important than the former, a global stabilization of the iron(II) HS state takes place. This is observed in the form of a residual HS fraction at very low temperature and a shift of T_c toward low temperatures. It should be noted that, in the case of the series $[\text{Fe}_x\text{Ni}_{1-x}]$, neither the HS state nor the LS state of iron(II) ions is stabilized by the presence of nickel(II) ions.²⁸

From the above considerations, it clearly appears that the relative sizes of the metal ions play a large part in dilution effects. However, for a given Fe(II)/M pair, these effects are also found to strongly depend on the nature of the complexes. In the case of $[\text{Fe}_x\text{Co}_{1-x}(\text{2-pic})_3]\text{Cl}_2\cdot\text{EtOH}$ for instance, there is neither residual LS form above ≈ 250 K nor residual HS form at very low temperature, whatever x may be.²⁰ On the other hand, regarding $\text{Fe}_x\text{Co}_{1-x}(\text{phen})_2(\text{NCS})_2$ (where phen = 1,10-phenanthroline), large amounts of residual LS form are observed well above T_c for low x values, while the residual HS form below ≈ 100 K does not differ significantly from that related to the pure iron species.^{27,35} It follows that other parameters than ionic radii do also influence dilution effects significantly. In particular, the response of the lattice to the stress resulting from the substitution of iron(II) ions by M ions and, therefore, the structure of the compounds, should play an important role.

In the present case, the metal ions are linked together through bridging ligands, defining a nearly two-dimensional polymer. Owing to the presumable softness of this structure, the local stresses induced by dilution are then expected to be readily absorbed through lattice strains.

Let us now consider the case of the nonpolymeric complexes $\text{Fe}_x\text{Co}_{1-x}(\text{phen})_2(\text{NCS})_2$. The structure of $\text{Fe}(\text{phen})_2(\text{NCS})_2$ in the crystalline form II has been reported.³⁶ The molecular packing may be described as sheets of molecules parallel to the a - b plane. The existence of "contacts" between atoms of neighboring molecules, viz. $\text{C}_{\text{phen}} - \text{C}_{\text{phen}}$ intrasheet contacts (several types) and $\text{C}_{\text{phen}} - \text{S}(\text{CN})$ intersheet contacts (one type), leads to definition of the metallic site as a "rigid box". So, this structure is expected to be stiffer than the previous one. The stabilization of the iron(II) LS form in the high-temperature range, observed for $x \leq 0.5$ when cobalt(II) ions are introduced,^{27,35} may then be accounted for by the fact that HS iron(II) ions, when they are mainly surrounded by slightly smaller cobalt(II) ions, are forced to undergo a HS to LS conversion. On the other hand, nothing prevents an iron(II) ion from remaining in the LS state when the major portion of its surroundings is composed of bulkier cobalt(II) ions, which may explain the fact that the residual HS fraction at low temperature does not vary noticeably with dilution.

The case of $[\text{Fe}_x\text{Co}_{1-x}(\text{2-pic})_3]\text{Cl}_2\cdot\text{EtOH}$ ²⁰ compounds can be considered as intermediate between the two previous cases: the relative softness of the lattice, resulting from the existence of a network of intermolecular hydrogen bonds, is then sufficient to keep iron(II) ions in their HS form in the high-temperature range, even for low x values, but it is not significant enough to lead to a stabilization of the HS form at low temperature. This

accounts for the completeness of HS to LS and LS to HS conversions, whatever x may be.

Thermodynamic Approach

We have already developed an adaptation of the model of Slichter and Drickamer³¹ to interpret the dilution effects in the mixed-crystal series $[\text{Fe}_x\text{Ni}_{1-x}]$.²⁸ Let us recall that, in this model, the solid mixture of HS and LS complexes which forms upon the spin transition is assumed to behave as a strictly regular solution. Consequently, its Gibbs free energy includes not only the intramolecular contributions of both spin forms, but also a term accounting for the mixing entropy and an interaction term of enthalpic origin.

In the case of $[\text{Fe}_x\text{Co}_{1-x}]$ compounds, the residual HS fraction at low temperature (r_{HS}) has to be introduced in the expression of the Gibbs free energy. With this aim in view, a number of iron(II) ions are assumed to be trapped in the HS state at any temperature, as a consequence of the local stresses exerted by cobalt(II) ions. So, N_A mononuclear entities of $[\text{Fe}_x\text{Co}_{1-x}]$ contain (1) xN_A [Fe] groups made up of $xn_{\text{HS}}N_A$ groups in the HS state, including $xr_{\text{HS}}N_A$ groups trapped in this state, and $x(1 - n_{\text{HS}})N_A$ groups in the LS state and (2) $(1 - x)N_A$ [Co] groups.

The relevant Gibbs free energy is then defined as

$$G = xn_{\text{HS}}G_{\text{HS}}^{\circ} + x(1 - n_{\text{HS}})G_{\text{LS}}^{\circ} + (1 - x)G_{\text{Co}}^{\circ} + x^2(n_{\text{HS}} - r_{\text{HS}})(1 - n_{\text{HS}})\Gamma + x(1 - x)n_{\text{HS}}\Gamma_{\text{HS/Co}} + x(1 - x)(1 - n_{\text{HS}})\Gamma_{\text{LS/Co}} - xn_{\text{HS}}TS_{\text{v}}^{\text{HS}}(x) - x(1 - n_{\text{HS}})TS_{\text{v}}^{\text{LS}}(x) - TS_{\text{mix}} \quad (5)$$

where G_{HS}° , G_{LS}° , and G_{Co}° are the standard Gibbs free energies of N_A entities [Fe] in the HS state (denoted $[\text{Fe}]_{\text{HS}}$) and in the LS state (denoted $[\text{Fe}]_{\text{LS}}$) and N_A entities [Co], respectively; Γ , $\Gamma_{\text{HS/Co}}$, and $\Gamma_{\text{LS/Co}}$ are parameters accounting for the interactions between the groups $[\text{Fe}]_{\text{HS}}$ and $[\text{Fe}]_{\text{LS}}$, $[\text{Fe}]_{\text{HS}}$ and [Co], and $[\text{Fe}]_{\text{LS}}$ and [Co], respectively. The latter parameters are of enthalpic origin. The residual HS fraction appears as a correction of the term related to the interaction between HS and LS iron(II) ions: this presupposes that the ions of this fraction, trapped in the HS state, do not take part in the interaction. $S_{\text{v}}^{\text{HS}}(x)$ and $S_{\text{v}}^{\text{LS}}(x)$ represent the differences between the entropies of vibrational origin relative to N_A entities $[\text{Fe}]_{\text{HS}}$ and $[\text{Fe}]_{\text{LS}}$ in the undiluted system and in the mixed system, respectively. S_{mix} stands for the mixing entropy and can be written as

$$S_{\text{mix}} = -R\{x(n_{\text{HS}} - r_{\text{HS}})\ln[x(n_{\text{HS}} - r_{\text{HS}})] + xr_{\text{HS}}\ln(xr_{\text{HS}}) + x(1 - n_{\text{HS}})\ln[x(1 - n_{\text{HS}})] + (1 - x)\ln(1 - x)\} \quad (6)$$

In what follows, eq 5 can be replaced by eq 7, where only the terms depending on n_{HS} have been retained:

$$G' = xn_{\text{HS}}[\Delta H^{\circ} - T\Delta S^{\circ}] + x^2(n_{\text{HS}} - r_{\text{HS}})(1 - n_{\text{HS}})\Gamma + x(1 - x)n_{\text{HS}}\Gamma_{\text{M}} - xn_{\text{HS}}T\Delta S_{\text{v}}(x) - TS_{\text{mix}} \quad (7)$$

Here $\Delta H^{\circ} = H_{\text{HS}}^{\circ} - H_{\text{LS}}^{\circ}$ and $\Delta S^{\circ} = S_{\text{HS}}^{\circ} - S_{\text{LS}}^{\circ}$ are the standard enthalpy and entropy changes associated with the spin conversion of N_A [Fe] entities in the pure iron compound and

$$\Gamma_{\text{M}} = \Gamma_{\text{HS/Co}} - \Gamma_{\text{LS/Co}} \quad (8)$$

$$\Delta S_{\text{v}}(x) = S_{\text{v}}^{\text{HS}}(x) - S_{\text{v}}^{\text{LS}}(x) \quad (9)$$

G' can also be written as

(35) Martin, J. P.; Zarembowitch, J., unpublished results.

(36) Gallois, B.; Real, J. A.; Hauw, C.; Zarembowitch, J. *Inorg. Chem.* **1990**, *29*, 1152.

$$G' = xn_{\text{HS}}[\Delta H(x) - T\Delta S(x)] + x^2(n_{\text{HS}} - r_{\text{HS}})(1 - n_{\text{HS}})\Gamma - TS_{\text{mix}} \quad (10)$$

where

$$\Delta H(x) = \Delta H^\circ + (1 - x)\Gamma_{\text{M}} \quad (11)$$

$$\Delta S(x) = \Delta S^\circ + \Delta S_{\text{v}}(x) \quad (12)$$

Equation 10 compares with the corresponding equation established by Slichter and Drickamer for $x = 1$, where G°_{LS} would be taken as the energy origin. Applying the equilibrium condition $(\partial G/\partial n_{\text{HS}})_{T,P,x} = (\partial G'/\partial n_{\text{HS}})_{T,P,x} = 0$ leads to

$$\ln\left[\frac{1 - n_{\text{HS}}}{n_{\text{HS}} - r_{\text{HS}}}\right] = \frac{\Delta H(x) + (1 + r_{\text{HS}} - 2n_{\text{HS}})\Gamma}{RT} - \frac{\Delta S(x)}{R} \quad (13)$$

and hence to

$$T = \frac{\Delta H(x) + (1 + r_{\text{HS}} - 2n_{\text{HS}})\Gamma}{\Delta S(x) + R \ln\left[\frac{1 - n_{\text{HS}}}{n_{\text{HS}} - r_{\text{HS}}}\right]} \quad (14)$$

from which it is easy to deduce the evolution of n_{HS} as a function of T . It should be noted that, in the case of highly diluted systems, the term including Γ in eq 13 can be neglected, which leads to eq 4.

Let us now consider the evolution of the parameters $\Delta H(x)$, $\Delta S(x)$, and Γ as a function of dilution.

Enthalpy Variation: $\Delta H(x) = \Delta H^\circ + (1 - x)\Gamma_{\text{M}}$. Owing to the relative sizes of cobalt(II), HS iron(II), and LS iron(II) ions, the interaction terms of enthalpic origin $\Gamma_{\text{HS/Co}}$ and $\Gamma_{\text{LS/Co}}$, involved in the expression of Γ_{M} (see eq 8), account for the destabilization of the HS and LS forms of iron(II), respectively. So, they are positive. Moreover, assuming they are mainly governed by the difference in radius of the two interacting ions, $\Gamma_{\text{HS/Co}}$ is then expected to be negligible compared with $\Gamma_{\text{LS/Co}}$. It follows that Γ_{M} should be negative and, consequently, that $\Delta H(x)$ should decrease linearly with x . The DSC data plotted in Figure 9 provide evidence for such a behavior.

Since the ionic radii of cobalt(II) and HS iron(II) are close to each other, $\Gamma_{\text{LS/Co}}$, and hence $|\Gamma_{\text{M}}|$, are expected to be of the same order of magnitude as $\Gamma_{\text{LS/HS}} = \Gamma$. Actually, the value of $|\Gamma_{\text{M}}|$ deduced from the calorimetric data, viz. $\approx 10 \text{ kJ}\cdot\text{mol}^{-1}$, is about twice the value of Γ (vide infra). This situation may be explained by the approximation involved in the above argument and/or by the fact that the experimental error on calorimetric data, which increases with iron(II) dilution, leads to underestimation of $\Delta H(x)$, and hence to overestimation of $|\Gamma_{\text{M}}|$.

Γ_{M} , which introduces a correction to the standard enthalpy change, plays a role similar to that of the term $\Delta = 2\Gamma(V_{\text{M}} - V_{\text{LS}})/(V_{\text{HS}} - V_{\text{LS}})$ ($V_{\text{M,LS,HS}}$ = unit-cell volumes of [M], [Fe]_{LS}, [Fe]_{HS} entities) in the lattice expansion model^{19–21,23} based on the so-called "sphere in a hole" model of Eshelby.³⁷ The values of this latter parameter were found, by Adler et al.,²¹ to be $\approx 8.4 \text{ kJ}\cdot\text{mol}^{-1}$ for $[\text{Fe}_x\text{M}_{1-x}(\text{2-pic})_3]\text{Cl}_2\cdot\text{CH}_3\text{OH}$ with $\text{M} = \text{Zn}$ or Co (the ionic radii of which are very close to each other, viz. 88 and 88.5 pm, respectively) and $\approx 10.8 \text{ kJ}\cdot\text{mol}^{-1}$ for $[\text{Fe}_x\text{Zn}_{1-x}(\text{2-pic})_3]\text{Cl}_2\cdot\text{C}_2\text{H}_5\text{OH}$. They are of the same order of magnitude as $|\Gamma_{\text{M}}|$ and are also found to be higher than the corresponding Γ value, estimated at $1.6 \text{ kJ}\cdot\text{mol}^{-1}$ for $[\text{Fe}_x\text{Zn}_{1-x}(\text{2-pic})_3]\text{Cl}_2\cdot\text{C}_2\text{H}_5\text{OH}$.

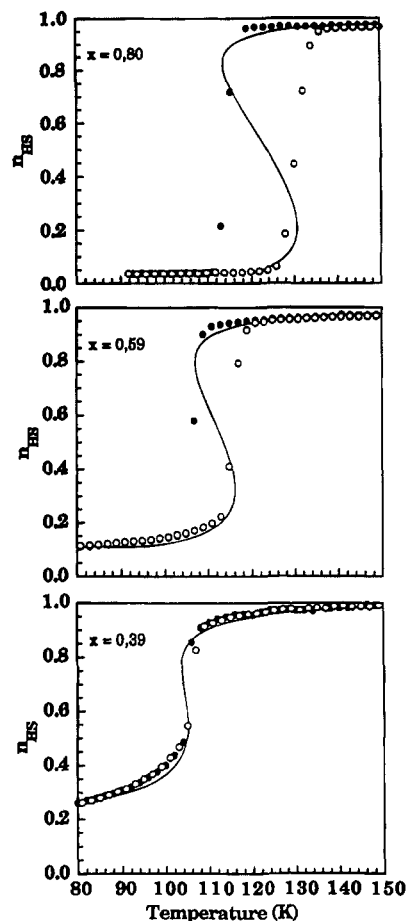


Figure 12. Experimental (●, in the cooling mode; ○, in the heating mode) and simulated (solid lines) n_{HS} vs T curves for some representative x values.

Entropy Variation: $\Delta S(x) = \Delta S^\circ + \Delta S_{\text{v}}(x)$. As reported earlier in the case of the mixed-crystal series $[\text{Fe}_x\text{Ni}_{1-x}]$,²⁸ the entropy change associated with the spin conversion depends on iron(II) concentration, as a consequence of the variation of its vibrational component with dilution. The same situation should occur here: owing to the coupling of metal–ligand vibrations which is likely to exist within the molecular equatorial plane, the frequencies of the Fe–N(btr) modes are expected to be all the more modified as the number of Co–N(btr) bonds in the vicinity of a given Fe–N(btr) bond increases. The resulting additional entropy variation, $\Delta S_{\text{v}}(x)$, is found to decrease with iron concentration, leading to a lowering of the total entropy change (see Figure 10).

Interaction Parameter Γ . The experimental n_{HS} vs T curves deduced from magnetic measurements have been quite properly simulated from eq 14, using the DSC data (ΔH and ΔS) and taking Γ as the variable. This can be observed in Figure 12 for a few x values. Regarding the calculated curves shown in this figure, it is worth noticing that, in the temperature range limited by the two vertical tangents which define the hysteresis loop, three solutions are found for n_{HS} : the two extreme ones correspond to the minima of G and represent stable or metastable states, while the intermediate one is associated with a maximum of G , and hence characterizes a state out of equilibrium.^{3,38}

The Γ values determined in the case of the pure iron complex and of the rather concentrated samples for which the contribution of cobalt ions to magnetic susceptibility is not too high compared to the contribution of iron(II) ions do not significantly differ.

(37) Eshelby, J. D. *Solid State Phys.* **1956**, *3*, 79.

(38) Zarembowitch, J.; Kahn, O. *New J. Chem.* **1991**, *15*, 181.

For instance, they are found to be 4.3, 4.2, and 4.8 $\text{kJ}\cdot\text{mol}^{-1}$ for $x = 1.00$, 0.80, and 0.59, respectively.

In the case of undiluted systems, the hysteresis was shown to vanish when $\Gamma = 2RT_c$.³¹ For mixed-crystal systems, it is easy to demonstrate that this condition becomes $\Gamma = 2RT_c/x$. Figure 4 shows that, in the series $[\text{Fe}_x\text{Co}_{1-x}]$, this situation occurs for $x \approx 0.37$ and $T_c \approx 102$ K, which leads to $\Gamma \approx 4.6$ $\text{kJ}\cdot\text{mol}^{-1}$. This value is in keeping with that previously obtained by the same procedure from the data related to the series $[\text{Fe}_x\text{Ni}_{1-x}]$, viz. 4.8 $\text{kJ}\cdot\text{mol}^{-1}$,²⁸ and with the values deduced from the simulation of n_{HS} vs T curves in the present work.

Conclusion

The phenomenological model used to account for the effects of dilution in the mixed-crystal series $[\text{Fe}_x\text{Co}_{1-x}]$ proves to reproduce the experimental spin-crossover curves quite properly. A similar conclusion was previously drawn in the case of the homologous series $[\text{Fe}_x\text{Ni}_{1-x}]$.²⁸ Taking into account the sizes of LS iron(II), HS iron(II), nickel(II), and cobalt(II) ions, as well as the crystal structure, leads to a satisfying interpretation

of the experimental data (in spite of the fact that that dilution effects are quite different in the two series), which points out the elastic origin of the interaction parameters.

Another important feature associated with dilution is the evolution of the vibrational component of the entropy change, resulting from the coupling of metal–ligand vibrations within the equatorial plane: ΔS varies from ≈ 76 $\text{J}\cdot\text{K}^{-1}\cdot\text{mol}^{-1}$ for $x = 1$ to 28 $\text{J}\cdot\text{K}^{-1}\cdot\text{mol}^{-1}$ ($[\text{Fe}_x\text{Co}_{1-x}]$) and 47 $\text{J}\cdot\text{K}^{-1}\cdot\text{mol}^{-1}$ ($[\text{Fe}_x\text{Ni}_{1-x}]$) for $x \approx 0.4$.

It should be noted that the agreement found in the present work between the calculated and experimental data is likely to largely result from the fact that the phenomenological model employed is specially suitable for this case. In particular, it leads to hysteresis loops with (more or less extended) *vertical* sections. Now, the spin transition of the pure iron species is particularly abrupt and, as far as a hysteresis effect is observed, i.e. for $x > 0.37$, the n_{HS} vs T curves present a discontinuity around the transition temperature (for $x = 0.39$, $\approx 50\%$ of the spin conversion still occurs within a temperature range as narrow as 3 K).